American Mineralogist, Volume 80, pages 297–304, 1995

The influence of excess alkalis on the viscosity of a haplogranitic melt

K.-U. Hess, D. B. Dingwell, S. L. Webb
Bayerisches Geoinstitut, Universität Bayreuth, 95440 Bayreuth, Germany

Abstract

The effect of the addition of 5, 10, and 20 wt% of the alkali oxides on the viscosity of a haplogranitic melt composition has been investigated at 1 atm and in the temperature range of 400–1650 °C. The high-temperature viscosity data were obtained with concentric cylinder viscometry and the low-temperature viscosity data using micropenetration viscometry. The combined data sets for low- and high-temperature viscosities have been fitted for each composition using the Tamann-Vogel-Fulcher (TVF) equation. The effect of alkali oxide on the viscosity of a haplogranite melt is extreme. The viscosity decreases with added alkali oxide content in a nonlinear fashion. The first few mole percent of alkali oxide added decreases viscosity several orders of magnitude, whereas subsequent addition of alkali oxide has a much smaller effect. The effects of each of the alkalis are broadly similar, implying that the structural role of the alkalis is common to all. In detail however, the viscosity of the strongly peralkaline melts investigated here increases with the size of the added alkali cation in the order Li < Na < K,Rb,Cs. This trend probably reflects a minor influence of the alkali-O bond strengths on the melt viscosity. This distinction of a dominant depolymerizing influence and a minor alkali specific bond-strength influence has important implications for the comparison of these data with those for the addition of other depolymerizing agents on the viscosity of haplogranitic melt (e.g., H_2O, F_2O_{-1}).

Introduction

Some of our most basic ideas on the structure of silicate melts arise from the composition dependence of the viscosity of these liquids. The notion of a network of SiO_2 with strong bridging bonds corresponding to its high viscosity (Brückner, 1970), the network-forming role of alkali aluminate complexes added to SiO_2 retaining relatively high viscosity (Riebling, 1966), and the strong depolymerization and decrease of viscosity accompanying the addition of network modifiers such as alkali oxides or H_2O to SiO_2 (Bockris et al., 1955) are but three examples.

Peralkalinity in igneous systems is a striking example of the third effect: the depolymerizing influence of alkalis in excess of Al on the viscosity of melts. Alkali excesses can yield agpaitic ratios up to 1.5 in certain voluminous members of intermediate to silicic volcanic systems, and even more peralkaline compositions might be expected in more restricted volumes because of crystal fractionation effects involving feldspars.

The viscous behavior of strongly peralkaline melts and, in particular, the individual role of alkali oxides on the viscosity of fully polymerized melts offer us an opportunity to accomplish both a theoretical and a practical goal in viscometry. The link between depolymerization and viscosity can be better defined by a sufficiently precise comparison of the individual effects of the alkali oxides. The combination of high- and low-temperature viscosity determinations of increasingly peralkaline melts allows us to identify the onset of significantly non-Arrhenian temperature dependence of viscosity and thereby the limits of applicability of extrapolations from high-temperature superliquidus viscosity calculation schemes (e.g., Bottinga and Weill, 1972; Shaw, 1972).

In the present study we have combined micropenetration and concentric cylinder viscometry to obtain relatively complete viscosity-temperature relationships for a series of peralkaline silicic melt compositions. The results indicate significantly non-Arrhenian behavior for all peralkaline compositions. Two effects are observed in the comparison of individual alkali oxide additions; a broadly similar strongly nonlinear decrease of viscosity with the addition of alkali oxide and a more subtle positive correlation between alkali cation size and viscosity (compared at constant number of moles of added alkali). These two effects appear to indicate a more complex behavior of depolymerizing agents on the viscosity of a fully polymerized melt than has been previously the case, and the alkali trend identified here poses questions for the roles of H_2O and F in similar melt systems.

Methods

For our investigations we have chosen as a base composition a haplogranitic melt composition (designated HPG8 by Holtz et al., 1992) which lies near the 1-kbar (P_{H_2O}) ternary minimum in the system SiO_2-$NaAlSi_3O_8$-$KAlSi_3O_8$, whose composition is given in Table 1. To this base composition we have added 5, 10, and 20 wt% alkali

0003–004X/95/0304–0297$02.00

TABLE 1. Compositions of melts in weight percent determined by ICP-AES

SiO_2	Al_2O_3	Na_2O	K_2O	Excess alkali oxide	Total	Excess mole fraction	Added alkali oxide
78.6 ± 0.4	12.5 ± 0.2	4.6 ± 0.3	4.2 ± 0.2	—	99.9	−0.003	—
73.2 ± 0.3	12.9 ± 0.3	4.3 ± 0.3	4.4 ± 0.2	4.9 ± 0.4	99.7	0.101	Li_2O
71.0 ± 0.9	11.4 ± 0.5	4.2 ± 0.6	4.0 ± 0.2	9.2 ± 0.3	99.8	0.180	
63.9 ± 0.3	9.1 ± 0.1	3.8 ± 1.0	3.4 ± 1.1	20.5 ± 0.2	100.7	0.345	
74.1 ± 0.4	11.7 ± 0.6	9.0 ± 0.2	4.4 ± 0.9	—	99.2	0.050	Na_2O
72.1 ± 0.2	10.9 ± 0.6	12.9 ± 0.5	3.8 ± 0.8	—	99.7	0.091	
62.4 ± 0.4	10.1 ± 0.3	23.5 ± 0.2	3.4 ± 0.2	—	99.4	0.204	
74.6 ± 0.8	11.8 ± 0.8	4.4 ± 0.8	9.2 ± 1.0	—	100.0	0.037	K_2O
71.2 ± 1.4	10.8 ± 0.4	4.3 ± 0.9	13.9 ± 0.3	—	100.2	0.081	
64.3 ± 0.2	9.6 ± 0.5	3.8 ± 0.5	22.4 ± 0.5	—	100.1	0.121	
74.2 ± 0.7	12.6 ± 0.4	4.8 ± 0.4	4.3 ± 0.2	5.2 ± 0.9	101.1	0.016	Rb_2O
69.7 ± 0.9	11.7 ± 0.5	4.4 ± 0.3	4.1 ± 0.2	8.7 ± 0.4	98.6	0.032	
64.2 ± 0.4	9.3 ± 0.3	3.9 ± 0.3	3.6 ± 0.5	19.5 ± 0.4	100.5	0.076	
74.2 ± 1.3	11.6 ± 0.7	4.6 ± 0.2	4.0 ± 1.3	4.0 ± 3.0	98.4	0.010	Cs_2O
71.2 ± 0.7	12.3 ± 0.3	4.4 ± 0.7	4.0 ± 0.2	8.6 ± 2.4	100.5	0.021	
62.6 ± 0.3	9.5 ± 0.9	4.3 ± 0.5	3.4 ± 1.0	18.6 ± 0.2	98.4	0.051	

Note: numbers quoted as uncertainties are in percent relative to the analyzed amount.

oxides. The compositions were deliberately chosen to provide for a compositional space of experimental data wider than that found in nature. The strength of such a compositional base lies in the fact that the framework of viscosity data provided by this set of compositions can be interpolated to provide estimates of the viscosities of liquid compositions and is still broad enough for us to speculate on the fundamental structural controls controlling viscous flow in silicate melts as a function of melt depolymerization.

The melts investigated in the present study were generated by direct fusion of powder mixes of oxides and carbonates at 1 atm and 1400–1650 °C. The fusions were performed in thin-walled Pt crucibles with a $MoSi_2$ box furnace. The partially fused products of this initial fusion were transferred in the crucibles to the viscometer furnace, and a stirring spindle was entered into the samples from above. The samples were fused for hours to days until inspection of the stirring spindle, removed periodically from the melt, indicated that the melts were homogeneous and bubble-free. The melts were removed from the furnace and allowed to cool in air in the Pt crucibles.

Cylinders (8 mm in diameter) were cored out of the cooled melt and sawed into disks 3 mm long. These disks were polished on one end and stored in a desiccator until they were used in micropenetration experiments. The remaining glass was remelted and used for the concentric cylinder experiments. Samples of each composition were analyzed by solution-based ICP-AES methods. The results of the bulk analyses are presented in Table 1. The content of H_2O was monitored for selected samples using FTIR. Investigated samples contained 100–200 ppm H_2O. We wish to emphasize that the volatility of the heavy alkalis is only a significant concern during the initial fusion of powder mixes, with their very large effective surface areas and locally extreme values of component activities. The analyses performed above were on the homogenized products of high-temperature fusions, and yet they indicate negligible volatilization. All subsequent handling of the samples involves far less volatility than these initial fusions, as has been demonstrated in the laboratory many times in the past. Our additional control on volatility is the drift check during viscosity measurements noted below. No volatility is indicated during the viscosity measurements.

The high-temperature viscosities were measured with a Brookfield HBTD (full-scale torque = 5.75×10^{-1} Nm) up to 1650 °C and rotation speeds of 0.5–50 rpm. This study used the spindle design of Dingwell and Virgo (1988). The apparatus, technique, and data reduction were described by Dingwell (1989). The viscosity can be determined in the range of 10^0–10^5 Pa·s. The measurement is relative, and all measurements are based on calibration with a NBS (NIST) standard reference material (SRM) 711 (lead silica glass). The concentric cylinder viscosity determinations have an accuracy of ± 0.05 $\log_{10}$ Pa·s. The technique includes a series of steps of temperature reduction followed by a reoccupation of the highest temperature condition to check for drift in viscosity reading due to volatilization or instrument drift. No such drift has been observed, indicating that the samples maintain compositional integrity during high-temperature viscometry.

The low-temperature viscosities were measured using a micropenetration technique. This involves determining the rate at which an Ir indenter under a fixed load moves into the melt surface. These measurements were performed in a BÄHR DIL 802 V vertical push-rod dilatometer. The sample is placed in a silica rod sample holder under an Ar gas flow. The indenter is attached to one end of an alumina rod, which is attached at the other end to a weight pan. The metal connection between the alumina rod and the weight pan acts as the core of a calibrated linear voltage displacement transducer (LVDT). The movement of this metal core as the indenter is pushed into the melt yields the displacement. The present system uses hemispherical Ir indenters with diameters of 2 mm

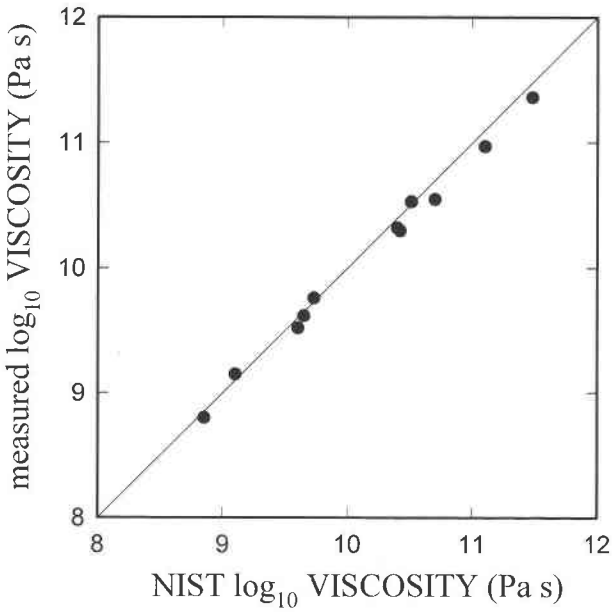

Fig. 1. The micropenetration viscometry method tested against SRM 711 lead-silicate glass. The viscosity of this reference glass can be reproduced to within 0.06 $\log_{10}$Pa·s at 1σ.

and a force of 1.2 N. The absolute shear viscosity is determined from

$$\eta = \frac{0.1875Pt}{r^{0.5}\alpha^{1.5}} \quad (1)$$

(Pocklington, 1940; Tobolsky and Taylor, 1963) for the radius of the half-sphere r, the applied force P, indent distance α, and time t ($t = 0$, $\alpha = 0$ upon application of the force). The measurements are performed over indentation distances of <100 μm. The technique yields an absolute determination of viscosity up to 1100 °C in the range of $10^{8.5}$–$10^{11.5}$ Pa·s. Viscosities determined on the NBS (NIST) standard SRM 711 have been reproduced within an error of ±0.06 log units (see Fig. 1).

Results and discussion

The results of the viscosity determinations are illustrated with the example of Li-bearing melts in Figure 2a and 2b. The concentric cylinder viscosity determinations, in the range of 10^{1}–10^{5} Pa·s (Fig. 2a), show a decreasing viscosity and temperature dependence of viscosity with increasing alkali content. The decrease is nonlinear, being more extreme at low excess alkali content. The micropenetration measurements (Fig. 2b) also reveal a nonlinear trend of decreasing viscosity with increasing alkali content, but the temperature dependence increases with added alkali. The high- and low-temperature viscosity data for all compositions are compiled in Tables 2 and 3 and Figure 3. These data have been fitted to the Tamann-Vogel-Fulcher equation (Eq. 2) to describe the temperature dependence of viscosity:

$$\log_{10}\eta = a + b/(T - c). \quad (2)$$

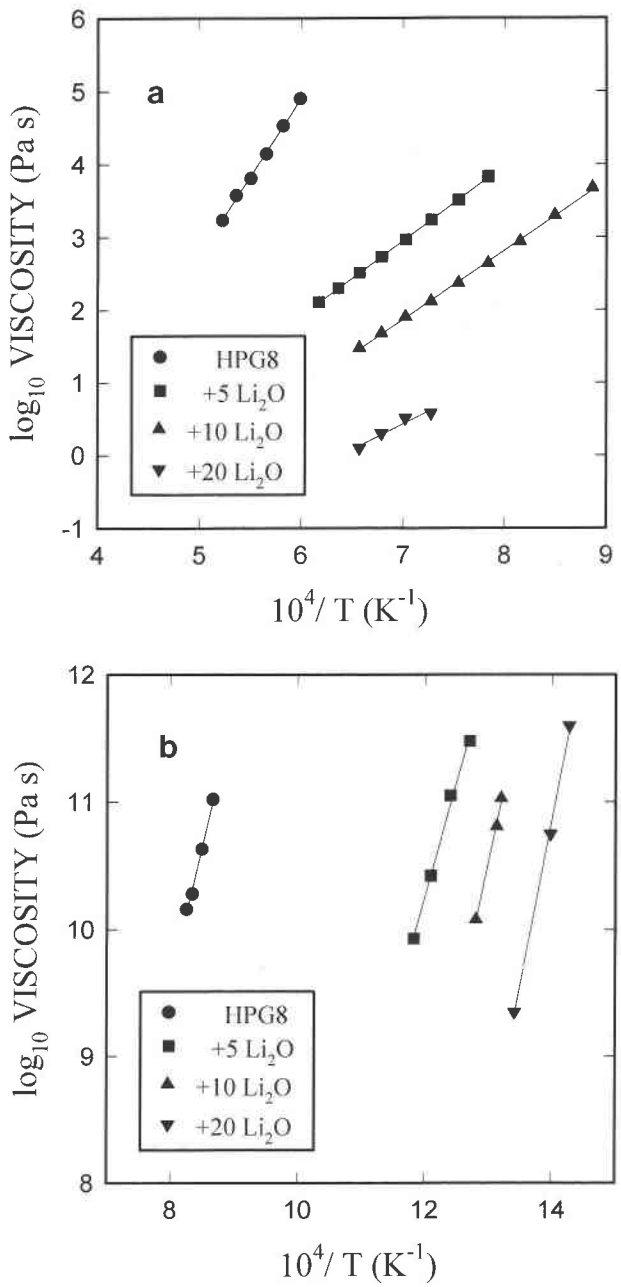

Fig. 2. **(a)** Concentric cylinder determination of the effect of added alkali oxide (Li_2O in this example) on the viscosity of a haplogranitic melt composition. Note the decrease in viscosity and activation energy with increasing alkali content. **(b)** Micropenetration viscometry determinations of the effect of added alkali oxide (Li_2O in this example) on the viscosity of a haplogranitic melt composition. Note the decrease in viscosity and increase in activation energy with increasing alkali content.

The results of the fits are presented in Table 4, and these fits are used as the basis for interpolation of viscosity data to construct the isothermal comparisons used below.

The viscosity-temperature relationship becomes in-

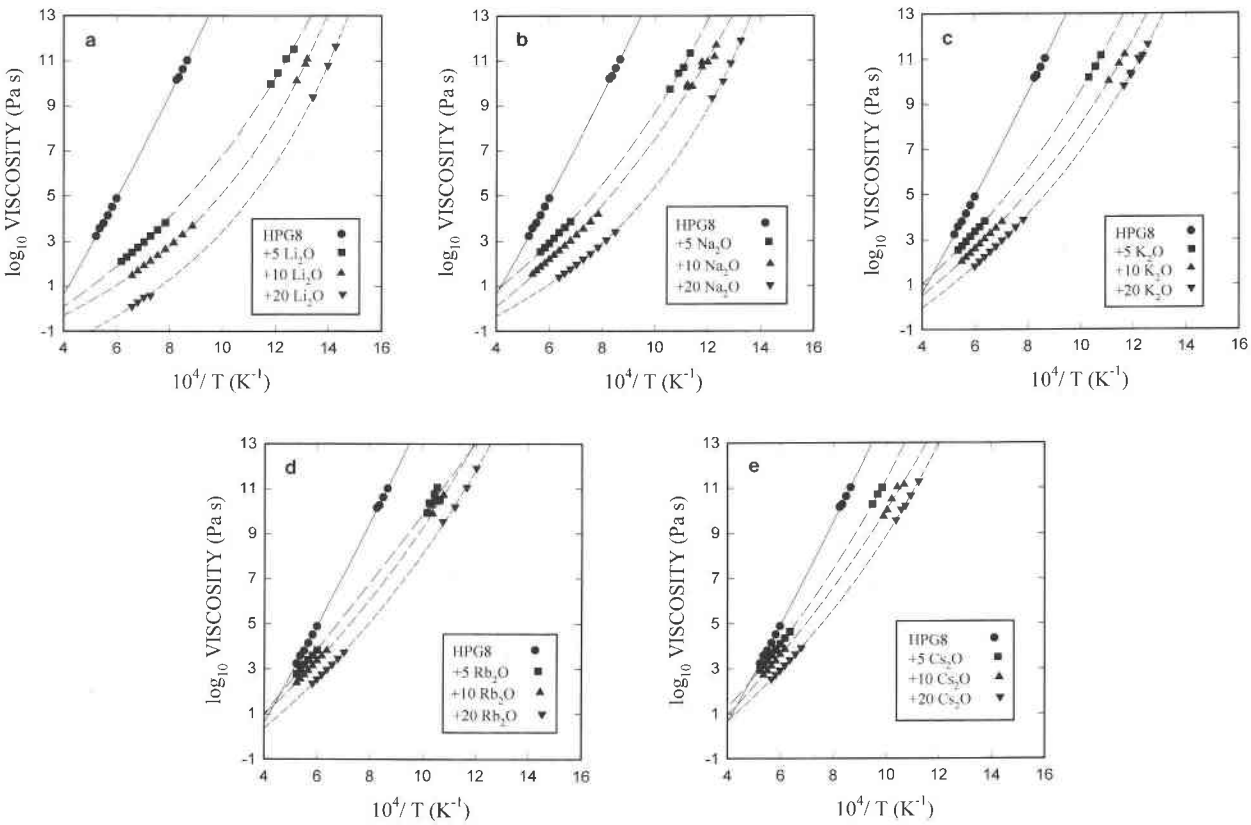

Fig. 3. The combined data set for all investigated compositions from both concentric cylinder and micropenetration viscometry. Note the increasingly non-Arrhenian nature of the viscosity-temperature relationships with increasing addition of alkali oxide **(a)** Li, **(b)** Na, **(c)** K, **(d)** Rb, and **(e)** Cs.

creasingly non-Arrhenian with increasing alkali content. The same trend is revealed for each of the alkalis to a varying degree, depending on the total molar percent of alkali in excess of the Al in the melts. Thus when an equal weight percent is added, the decrease in viscosity due to the addition of alkali oxide increases in the order Cs < Rb < K < Na < Li.

Comparison of the effects of the alkali oxides on a molar basis is illustrated in Figure 4a and 4b for two isotherms, 1300 and 800 °C. The molar fraction of excess alkali oxide was calculated by casting the analytical data of Table 1 into molar oxide components and then subtracting the analyzed Al_2O_3 value from the sum of the alkali oxides, the remainder being set equal to the mole fraction of excess alkali oxide. In this way any deviation from stoichiometry in the HPG8 composition in terms of the critical alkali-Al ratio is corrected. Figure 4 reveals that, at both 1300 and 800 °C, the effects of the individual alkali oxides on the viscosity of the haplogranitic melt are quite similar. The decrease in viscosity is a strongly nonlinear function of the mole fraction of excess alkali at both 800 and 1300 °C. The magnitude of the decrease and the nonlinearity with respect to mole fraction of excess alkali oxide both increase with decreasing temperature of the isothermal comparisons. At 800 °C a distinction can be made between the viscosity-composition trends of the light alkalis such that the viscosities of the peralkaline melts compared at constant mole fraction of added alkali oxides reveal the trend Cs,Rb,K > Na > Li. This distinction reaches a value of approximately 0.5 $\log_{10}$Pa·s between Li and Na (at a mole fraction of excess alkali oxide = 0.2). In contrast, the effect of adding this amount of alkali oxide to the haplogranite at the same temperature is a decrease of some 8 $\log_{10}$Pa·s. Clearly the latter effect dominates, but the distinction of an alkali-specific effect is important for further comparisons, as emphasized below.

The degree of non-Arrhenian behavior of the presently investigated melts is a point of obvious concern for predictive models and a potential source of structural information on these melts. We have quantified the degree of non-Arrhenian behavior with the empirical parameter, N:

$$N = c/T_N \tag{3}$$

where c is the parameter from Equation 2 and T_N is the temperature at which the viscosity equals 10^{12}Pa·s. This formulation of N quantifies the degree of non-Arrhenian temperature dependence of viscosity, the "fragility" (Angell, 1984) of silicate melt viscosities.

The parameter, N, plotted in Figure 5, varies system-

TABLE 2. Micropenetration viscosity data ($\log_{10}$ Pa·s)

T (±0.5 °C)	$\log_{10}\eta$ (±0.06)	Comp./samp.	T (±0.5 °C)	$\log_{10}\eta$ (±0.06)	Comp./samp.
572.2	9.93	Li5/1	712.8	9.93	Rb5/1
554.0	10.42	Li5/1	696.6	10.30	Rb5/1
533.4	11.05	Li5/1	682.4	10.50	Rb5/1
514.3	11.48	Li5/1	677.1	11.07	Rb5/1
507.8	10.08	Li10/1	705.4	10.37	Rb5/2
488.4	10.81	Li10/1	667.8	10.52	Rb5/2
484.4	11.03	Li10/1	686.8	10.77	Rb5/2
472.6	9.35	Li20/1	692.6	9.90	Rb10/1
442.2	10.75	Li20/1	670.6	10.42	Rb10/1
427.6	11.60	Li20/1	655.7	10.72	Rb10/1
674.5	9.74	Na5/1	657.7	9.55	Rb20/1
646.5	10.45	Na5/1	619.6	10.20	Rb20/1
630.5	10.70	Na5/1	585.2	11.07	Rb20/1
610.3	11.35	Na5/1	558.8	11.93	Rb20/1
618.8	9.82	Na10/1	784.0	10.26	Cs5/1
576.7	10.74	Na10/1	762.5	10.70	Cs5/1
561.4	10.95	Na10/1	744.2	11.00	Cs5/1
544.0	11.18	Na10/1			
604.4	9.86	Na10/2	739.5	9.72	Cs10/1
618.0	9.93	Na10/2	724.5	10.00	Cs10/1
576.8	10.95	Na10/2	707.9	10.48	Cs10/1
539.5	11.7	Na10/2	687.8	11.02	Cs10/1
549.5	9.35	Na20/1	664.9	11.13	Cs10/1
522.5	10.10	Na20/1	692.6	9.57	Cs20/1
504.4	10.90	Na20/1	673.5	10.04	Cs20/1
482.4	11.90	Na20/1	660.3	10.21	Cs20/2
696.2	10.16	K5/1	642.9	10.65	Cs20/2
672.6	10.65	K5/1	618.6	11.27	Cs20/2
654.1	11.15	K5/1	938.8	10.16	HPG8/1
629.5	10.01	K10/1	925.7	10.28	HPG8/1
598.5	10.78	K10/1	881.7	11.02	HPG8/1
582.4	11.20	K10/1	905.0	10.63	HPG8/1
584.9	9.80	K20/1			
542.9	10.95	K20/1			
535.4	11.15	K20/1			
522.9	11.65	K20/1			
545.8	11.02	K20/2			
565.8	10.28	K20/2			
566.6	10.36	K20/2			

Note: comp./samp. = composition and sample.

TABLE 4. Fit parameters for the Tamann-Vogel-Fulcher equation

	a ($\log_{10}$Pa·s)	b ($\log_{10}$ Pa·s/K)	c (K)	N
5Li	−2.77(0.29)	6084(446)	364.1(23.3)	0.47
10Li	−2.26(0.07)	4015(800)	455.0(4.6)	0.62
20Li	−3.45(0.19)	3822(230)	446.7(12.7)	0.64
5Na	−2.41(0.23)	6845(416)	384.7(22.4)	0.45
10Na	−3.21(0.46)	7155(797)	333.7(40.6)	0.41
20Na	−2.38(0.13)	4178(152)	463.0(8.6)	0.61
5K	−2.64(0.18)	7855(357)	356.2(18.7)	0.40
10K	−2.75(0.07)	7038(121)	351.3(6.4)	0.42
20K	−2.97(0.19)	6264(296)	367.4(15.2)	0.47
5Rb	−4.37(2.72)	13060(7033)	83.93(312.8)	0.01
10Rb	−2.84(0.18)	8413(366)	307.7(19.3)	0.35
20Rb	−3.08(0.32)	7512(557)	330.0(27.8)	0.40
5Cs	−3.30(0.18)	9951(403)	323.0(19.3)	0.33
10Cs	−3.58(0.98)	10140(2144)	255.3(102.4)	0.28
20Cs	−2.87(0.19)	7648(349)	351(18.1)	0.41
HPG8	−7.32(0.83)	18850(2255)	129(77.5)	0.12

Note: the numbers in parentheses represent one standard error, which is equal to one standard deviation divided by the square root of the number of samples.

atically with melt polymerization. As can be seen in Figure 5, the molar comparison of alkali oxide additions generates a single trend. Thus the parameter N effectively accounts for the degree of fragility and indicates that the structural effect of adding the nonbridging O atoms associated with alkali oxide incorporation into the melt structure is, for the present set of data, sufficient to account for the non-Arrhenian behavior.

At this point we wish to draw attention to an important point concerning normalizations such as that provided by Equation 3. The N normalization can only be applied to melt viscosity-temperature relationships for which the parameter a (Eq. 2) is constant. The argument can be made that all viscosity-temperature relations, if sufficiently well constrained, must have an intercept value near 10^{-3}–10^{-5} Pa·s because this viscosity corresponds to a vibrational relaxation time. To the extent that such intercept values are returned by fits to our depolymerized melts and that the variation in a obtained is small, the N normalization is robust and should be acceptable for empirical predictive purposes. We caution, however, against the use of the N parameter in circumstances where insufficient data are available to demonstrate the validity

TABLE 3. Concentric cylinder viscometry data ($\log_{10}$ Pa·s)

T (°C)	5Li	10Li	20Li	5Na	10Na	20Na	5K	10K	20K	5Rb	10Rb	20Rb	5Cs	10Cs	20Cs	HPG8
1643	—	—	—	—	—	—	—	—	—	2.77	2.38	—	2.94	—	—	3.24
1594	—	—	—	—	1.53	—	2.54	—	—	2.95	2.55	—	3.14	2.71	—	3.58
1544	—	—	—	—	1.69	—	2.72	2.03	—	3.19	2.73	—	3.37	2.90	—	3.81
1495	—	—	—	2.53	1.85	—	2.92	2.21	—	3.40	2.92	—	3.60	3.12	2.53	4.15
1446	—	—	—	2.72	2.01	—	3.14	2.39	—	3.60	3.14	2.36	3.84	3.34	2.73	4.53
1397	—	—	—	2.91	2.19	—	3.36	2.60	1.82	3.84	3.36	2.55	4.10	3.63	2.93	4.90
1348	2.11	—	—	3.14	2.38	—	3.57	2.80	2.04	—	3.57	2.76	4.36	3.86	3.15	—
1298	2.30	—	—	3.38	2.58	1.40	3.82	3.03	2.25	—	3.82	2.97	4.65	—	3.40	—
1249	2.51	1.48	0.10	3.61	2.79	1.58	—	3.27	2.48	—	—	3.20	—	—	3.65	—
1200	2.73	1.68	0.30	3.87	3.02	1.77	—	3.51	2.71	—	—	3.47	—	—	3.92	—
1151	2.97	1.91	0.51	—	3.28	1.98	—	3.79	2.97	—	—	3.75	—	—	—	—
1102	3.24	2.12	0.58	—	3.54	2.21	—	—	3.24	—	—	—	—	—	—	—
1052	3.51	2.37	—	—	3.86	2.46	—	—	3.56	—	—	—	—	—	—	—
1003	3.83	2.64	—	—	4.19	2.74	—	—	3.89	—	—	—	—	—	—	—
954	—	2.94	—	—	—	3.07	—	—	—	—	—	—	—	—	—	—
905	—	3.30	—	—	—	3.42	—	—	—	—	—	—	—	—	—	—
856	—	3.68	—	—	—	—	—	—	—	—	—	—	—	—	—	—

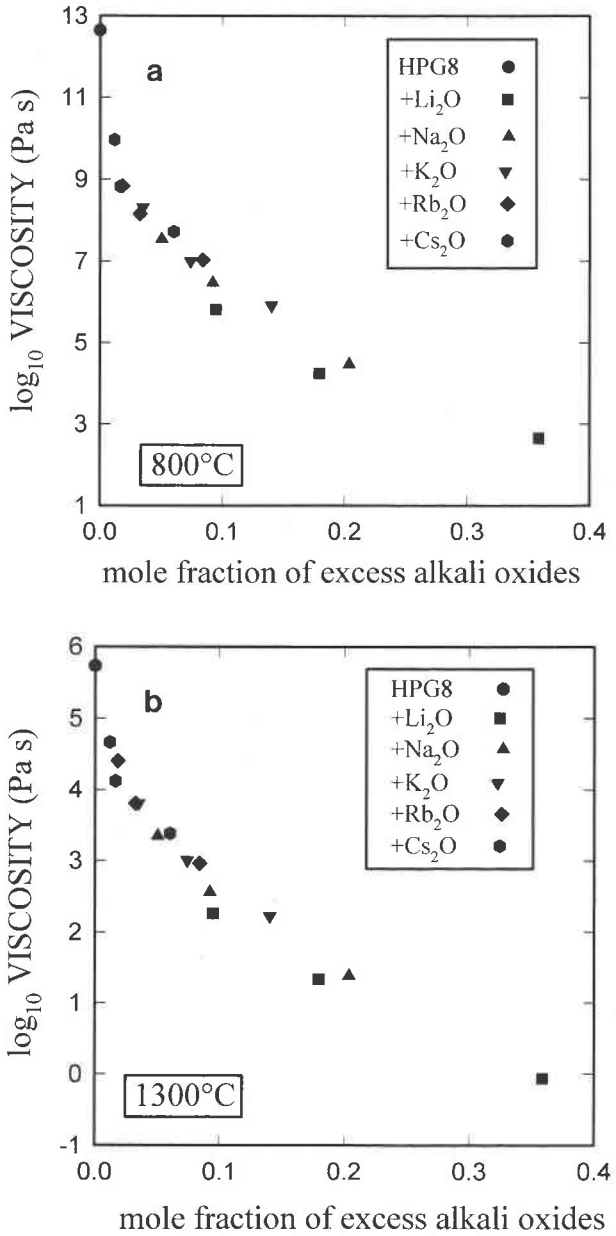

Fig. 4. A molar comparison of the effects of the alkali oxides on the viscosity of a haplogranitic melt at temperatures of 800 °C **(a)** and 1300 °C **(b)**. The data are interpolated using the TVF fits of Table 4. Note that the effects of all the alkalis are very similar. At 800 °C, however, a slight cation-specific dependence of viscosity on composition is observed such that viscosity, at constant added alkali oxide content, decreases in the order Cs_2O, Rb_2O, $K_2O > Na_2O > Li_2O$.

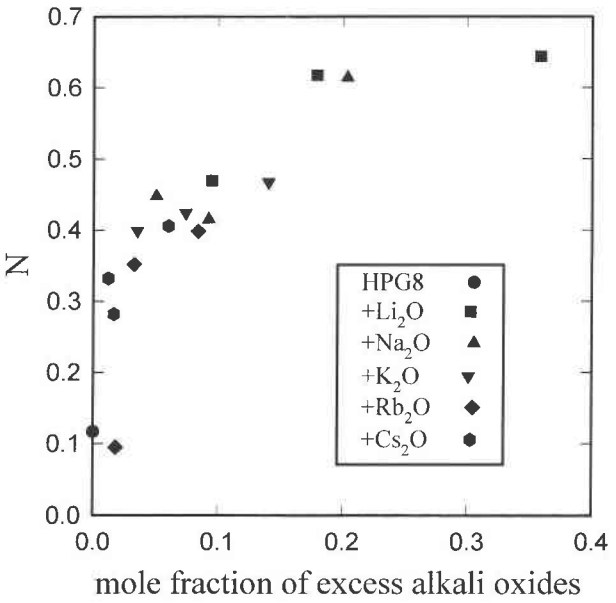

Fig. 5. The parameter *N*, describing the degree of non-Arrhenian temperature dependence of the viscosity of the investigated melts, plotted vs. the mole fraction of added alkali oxide.

of the assumption that the intercept value in the Arrhenian plot has such a value.

Comparison with H_2O and F

The comparison of the influences of excess alkalis and that of H_2O on the properties and structure of silicate melts has been performed several times in the past. In the case of viscosity, this comparison was made by Shaw (1963). He compared his data for the viscosities of rhyolites containing 4–6 wt% H_2O at 2000 bars and 700–900 °C with the then existing data for melt viscosities along the SiO_2-Na_2O join (Bockris et al., 1955). That comparison tested the hypothesis that H_2O and excess alkalis behave similarly in the silicate melt structure. The qualitative effects of H_2O on the viscosity of the rhyolite melt (i.e., strongly nonlinear decrease in viscosity and activation energy) were indeed reproduced by the SiO_2-Na_2O system. Thus the conclusion drawn by Shaw (1963) was that the structural roles of H_2O and excess alkalis are similar. The comparison possible at that time contained a number of unavoidable shortcomings, which are partly resolved by more recent and the present work. First, the viscosities of the base compositions for the comparison, a dry rhyolite and SiO_2 were poorly constrained. The SiO_2 viscosity was and is extremely difficult to specify because of the strong influence of impurities in the parts per million range. Additionally, the two melt compositions, although both believed to be structurally tectosilicate on the basis of their stoichiometry, are not equivalent; moreover, the viscosities of the two melts, rhyolite and SiO_2, are very different.

The second problem involved the calculation of the influence of H_2O on the melt viscosity in terms of a complete dissociation of H_2O in the melt. We now know that the dissociation of H_2O in silicic melts is far from complete, being instead a complex function of composition, temperature, and possibly pressure (Stolper, 1982; Dingwell and Webb, 1990; Zhang et al., 1991). Accordingly, a comparison of the structural roles of H_2O and excess

alkalis should include our best estimate of the dissociated, depolymerizing component (cf. Kohn et al., 1989) in the melt. Stolper (1982) drew attention to this point when he demonstrated a correlation between OH content of glass and melt viscosity. In essence he suggested that the nonlinearity in viscosity reduction was a consequence of the nonlinear variation of melt OH content with total H_2O content. In presenting a comparison of the effects of F and H_2O on melt viscosity, Dingwell (1987) raised the point that other structural components (e.g., the alkalis, F), thought to be completely dissociated in the melt structure, also demonstrate a strongly nonlinear dependence of viscosity on concentration of the added component. Thus assigning the nonlinearity in viscosity-concentration relations to the equilibrium between OH and molecular H_2O seemed problematic. Finally, White and Montana (1990) showed that CO_2 and H_2O have similar effects on melt viscosities at high temperature and pressure.

A third complication in the comparison involves the intrinsic effect of pressure. The viscosity data for H_2O-bearing melts are of necessity all obtained at elevated pressure, whereas the peralkaline viscosity data are obtained at 1 atm. We now know from the available data that the effect of pressure on the viscosity of both dry and wet melts is significant but not large enough to invalidate conclusions based on a comparison over a pressure range of 1–2 kbar (Scarfe et al., 1987; Dingwell, 1987; White and Montana, 1990).

The data from this study are compared in Figure 6 with data on the effects of H_2O (Shaw, 1972) and F (Dingwell et al., 1993) on the viscosity of haplogranitic melt. The effect of F, cast as the component F_2O_{-1}, lies within the curves illustrated for the alkalis. Two curves for H_2O are portrayed in Figure 6. The upper curve is plotted on the basis of total added H_2O. This curve can also be seen to lie within the trend of the family of curves for individual alkali oxides from this study. We seem forced to draw the general conclusion that the effects of H_2O, F and excess alkalis are very similar. As noted above, it has been speculated that the speciation of H_2O should play a role in determining the effect H_2O has on the transport and equilibrium properties of silicate melts, and that the role of molecular H_2O in influencing viscosity can be considered negligible. If we try to rationalize the effect of H_2O on viscosity in terms of the amount of OH in the melt rather than total added H_2O, we obtain the lower H_2O curve in Figure 6. The proportion of H_2O dissolved as OH is used as the molar addition of H_2O value for the ordinate. The calculation involves a correction of the quenched-in OH content of a rhyolitic melt with the temperature dependence of OH content estimated from kinetic analysis of speciation data (Dingwell and Webb, 1990; Ihinger, 1991). The lower H_2O curve in Figure 6 falls well below the curves for the alkali oxides because fully 50% of the dissolved H_2O is believed to be molecular H_2O at these concentrations and temperatures. This lower H_2O curve expresses the assumption that molecular or physically dissolved H_2O in silicate melts has no effect on melt viscosity. The addition of OH then to the structure of the haplogranitic melt appears, on the basis of Figure 6, to have a much larger effect than that of the added alkali oxides.

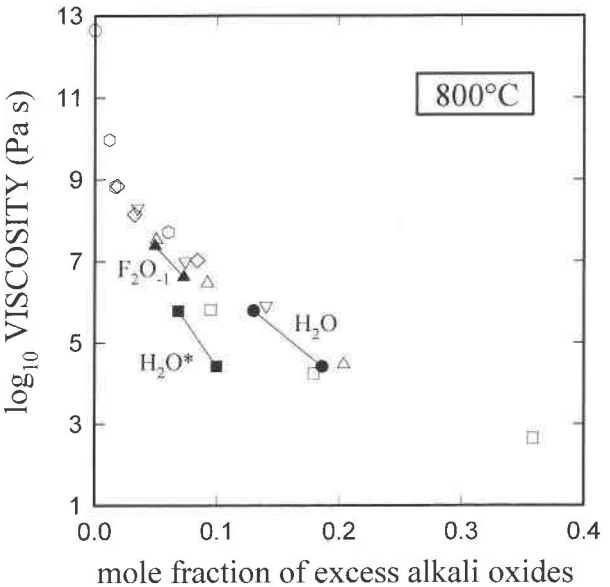

Fig. 6. Comparison of the effect of added alkali oxides on the viscosity of HPG8 melt (this study) with the effect calculated for H_2O on HPG8 melt using the method of Shaw (1972). The curves for H_2O are very similar to those for the alkali oxides. The curve labeled with an asterisk is the effect of H_2O on viscosity where the value of added H_2O is calculated on the basis of an estimate of the dissociated, chemically dissolved OH groups in the melt.

Although to a first approximation we may appear with this calculation of speciation to have removed the systematic trends of the alkali and H_2O effects (upper H_2O curve) in Figure 6, in detail this may not be the case. Remembering that the individual alkali oxides demonstrate, at constant mole fraction of added alkali oxide, a clear trend of decreasing viscosity in the order Cs,Rb,K > Na > Li, it is consistent to interpret the trend of decreasing viscosity as continuing to H. Quantification of this trend is difficult. We must return to the question of which atomic, ionic, or bulk parameter provides a useful scale for relating the effects of nonbridging O atoms related to alkalis and H atoms in the silicate melt structure. Clearly we are left with the old problem of how to extrapolate to H. A preferred comparison (e.g, Dingwell and Virgo, 1988) would be one that rationalizes the contributions of the alkali oxides and dissociated H_2O to bulk thermodynamic properties of the melt, i.e., to the enthalpy and configurational entropy (e.g., Richet, 1984). This is difficult, however, in the absence of sufficient data on both H_2O-bearing melts and peralkaline melts. Using the present data we can state that a comparison of H_2O, F, and alkalis, on the basis of melt depolymerization yields the conclusion that H_2O is as effective as the other completely dissociated components in reducing viscosity. If

the fraction of H_2O inferred (on the basis of infrared spectroscopy) to be present as molecular H_2O is subtracted, then the effect of H_2O on melt viscosity is much larger than that of F and the alkalis. The latter conclusion is consistent with the alkali size dependence of the relative viscosities of the peralkaline melts observed here.

Acknowledgments

We wish to thank Hubert Schulze, Anna Dietel, Georg Hermannsdörfer, and Detlef Krauße for technical and analytical assistance. Discussions with Nick Bagdassarov have been helpful. This work was supported by a grant of the Deutsche Forschungsgemeinschaft Gerhard-Hess-Programm (Di 431/3-1) to D.B.D.

References cited

Angell, C.A. (1984) Strong and fragile liquids. In K.L. Ngai and G.B. Wright, Eds., Relaxations in complex systems, p. 3–11. National Technical Information Service, U.S. Department of Commerce, Springfield, Virginia.

Bockris, J.O'M., MacKenzie, J.D., and Kitchener, J.A. (1955) Viscous flow in silica and binary silicates. Transactions of the Faraday Society, 51, 1734–1748.

Bottinga, Y., and Weill, D.F. (1972) The viscosity of magmatic silicate liquids: A model for calculation. American Journal of Science, 277, 438–475.

Brückner, R. (1970) Properties and structure of vitreous silica I. Journal of Non-Crystalline Solids, 5, 123–175.

Dingwell, D.B. (1987) Melt viscosities in the system $NaAlSi_3O_8$-H_2O-F_2O_{-1}. In B.O. Mysen, Ed., Magmatic processes: Physicochemical principles. The Geochemical Society Special Publication, 1, 423–433.

——— (1989) Shear viscosities of ferrosilicate liquids. American Mineralogist, 74, 1038–1044.

Dingwell, D.B., and Virgo, D. (1988) Melt viscosities in the Na_2O-FeO-Fe_2O_3-SiO_2 system and factors controlling the relative viscosities of fully polymerized silicate melts. Geochimica et Cosmochimica Acta, 152, 395–403.

Dingwell, D.B., and Webb, S.L. (1990) Relaxation in silicate melts. European Journal of Mineralogy, 12, 427–449.

Dingwell, D.B., Knoche, R., and Webb, S.L. (1993) The effect of P_2O_5 on the viscosity of a haplogranitic melt. European Journal of Mineralogy, 5, 133–140.

Holtz, F., Behrens, H., Dingwell, D.B., and Taylor, R.P. (1992) Water solubility in aluminosilicate melts of haplogranitic compositions at 2 kbar. Chemical Geology, 196, 289–302.

Ihinger, P.D. (1991) An experimental study of the interaction of water with granitic melt, 190 p. Ph.D. thesis, California Institute of Technology, Pasadena, California.

Kohn, S., Dupree, R., and Smith, M.E. (1989) A multinuclear magnetic resonance study of the structure of hydrous albite glasses. Geochimica et Cosmochimica Acta, 53, 2925–2935.

Pocklington, H.C. (1940) Rough measurement of high viscosities. Proceedings of the Cambridge Philosophical Society, 36, 507–508.

Richet, P. (1984) Viscosity and configurational entropy in silicate melts. Geochimica et Cosmochimica Acta, 48, 471–483.

Riebling, E.F. (1966) Structure of sodium aluminosilicate melts containing at least 50 mole % SiO_2 at 1500 °C. Journal of Chemical Physics, 44, 2857–2865.

Scarfe, C.M., Mysen, B.O., and Virgo, D. (1987) Pressure dependence of the viscosity of silicate melts. In B.O. Mysen, Ed., Magmatic Processes: Physicochemical principles. Geochemical Society Special Publication, 1, 59–67.

Shaw, H.R. (1963) Obsidian-H_2O viscosities at 1000 and 2000 bars in the temperature range 700 ° to 900 °C. Journal of Geophysical Research, 68, 6337–6343.

——— (1972) Viscosities of magmatic liquids: An empirical method of prediction. American Journal of Science, 272, 870–893.

Stolper, E.M. (1982) Water in silicate glasses. Contributions to Mineralogy and Petrology, 104, 142–162.

Tobolsky, A.V., and Taylor, R.B. (1963) Viscoelastic properties of a simple organic glass. Journal of Physical Chemistry, 67, 2439–2442.

White, B.S., and Montana, A. (1990) The effect of H_2O and CO_2 on the viscosity of sanidine liquid at high pressures. Journal of Geophysical Research, 95, 15683–15693.

Zhang, Y., Stolper, E.M., and Wasserburg, G.J. (1991) Diffusion of water in rhyolitic glasses. Geochimica et Cosmochimica Acta, 55, 441–456.

Manuscript received May 18, 1994
Manuscript accepted November 10, 1994